51st AIAA Aerospace Sciences Meeting including the New Horizons Forum and Aerospace Exposition
07 - 10 January 2013, Grapevine (Dallas/Ft. Worth Region), Texas

AIAA 2013-0076

Parameter-free Shock Detector and High Order Hybrid Algorithm for Shock/Complex Flowfield Interaction

Yiqing Shen* Kai Cui Guowei Yang

LHD, Institute of Mechanics, Chinese Academy of Sciences,
100190, Beijing, China

Gecheng Zha†
Dept. of Mechanical and Aerospace Engineering, University of Miami
Coral Gables, Florida 33124, USA

Abstract

In order to accurately simulate the interaction of shock wave/complex flows, hybrid schemes combining a compact scheme and weighted essentially non-oscillatory(WENO) scheme are beneficial, in particular due to the high order low dissipation schemes used in smooth regions. For a hybrid scheme, there are two key issues, one is how to detect the discontinuity, the other is how to choose the high order low dissipation scheme to ensure the accuracy, robustness and efficiency. In this paper, a shock detecting method without any artificial parameter is proposed using the definition of the derivative. Based on this shock detecting method, a high order accuracy low dissipation shock-capturing algorithm is constructed. Numerical examples show that the shock detecting method and the hybrid algorithm are accurate, efficient and robust.

1 Introduction

With the increasing research and application of computational fluid dynamics (CFD) in compressible flows, it is desirable that the numerical methods of CFD have both the properties of capturing discontinuities such as the shock waves with monotone profiles and high order low dissipation in smooth regions. However, these two properties are often conflicting. Capturing shock wave requires numerical dissipation, but if the numerical dissipation is excessive, it may overwhelm the actual physical diffusion. Researchers thus propose the hybrid schemes combining shock-capturing schemes and high-order accuracy low dissipation schemes, i.e. near shock wave regions, the shock-capturing schemes are used, while in smooth regions, the high-order low dissipation schemes are used. An important and challenge issue is: how to detect a shock accurately and efficiently.

Adams and Shariff[1] used a local maximum condition to detect the shock and proposed a hybrid scheme of ENO scheme and compact difference scheme. Pirozzoli[2] used the first order difference of three neighboring interface to switch the fluxes of WENO scheme and compact difference scheme. Ren et al.[3] developed a weighted WENO-compact hybrid scheme, the abrupt transition from one sub-scheme to another is avoided. Zhou et al.[4] followed the hybridization procedure of Ren et al[3], constructed the hybrid scheme of WENO and compact upwind scheme in which free parameters are optimized for higher spectral resolution. Shen et al.[5] treated the discontinuity as an internal boundary, proposed the finite

* yqshen@imech.ac.cn
† AIAA Associate Fellow, gzha@miami.edu

compact (FC) scheme, and constructed the FC-TVD scheme, FC-ENO scheme, and used an improved limiter as the shock detector to develop the hybrid FC-WENO scheme[6]. Numerical results show that these hybrid schemes have the ability of capturing shock waves essentially with no oscillation, and have the corresponding high order accuracy similar to the compact scheme in smooth region. Their limitation is that the artificial, problem-dependent parameters are introduced to detect the shock position.

Hill and Pullin[7] used the smoothness indicator of WENO scheme to develop the hybrid scheme of the tuned central-difference (TCD) scheme and WENO scheme. Pantano[8] applied a pressure and density curvature based discontinuity detection crierion to switch schems from TCD to WENO around shocks. Costa and Don[9] developed the hybrid central difference and WENO scheme, Hartens multi-resolution algorithm[10] is used to switch two different schemes.

Another category numerical methods is to combine the high order accuracy low diffusion scheme with the high order filters. For example, Yee et al.[11] used the non-dissipative fourth- or higher-order compact and non-compact differencings as the base schemes, an artiticial compression method switch is used to signal the appropriate amount of TVD or ENO types of characteristic based numerical dissipation, this term acts as a characteristic filter to minimize numerical dissipation for the overall scheme. Yee and Bjogreen[12] developed multiresolution wavelet decomposition of the computed flow data as sensors for adaptive numerical dissipative control, where a experiential Lipschitz exponent is needed. Bogey et al.[13] developed a shock-capturing methodology based on an adaptive spatial filtering, it applys a background selective filtering at each mesh point and a shock-capturing filtering around discontinuities. Based on the order analysis, Darian et al.[14] designed a shock detecting sensor for switching between a second-order and higher-order filter. For the above mentioned methods, either the central-WENO hybrid schemes, or the high order accuracy low dissipation scheme combined with the filters, they need an artificial (experiential), problem-dependent parameter to determine whether the numerical dissipation is necessary for capturing shocks. This greatly limits the applications of those numerical methods.

To develop parameter free hybrid schemes, Shen and Zha[15] proposed a lemma based on the WENO smoothness indicators of Jiang and Shu[16] and Borges et al.[17] to detect shock regions and a class of generalized finite compact difference schemes. Shen et al.[18] compared the performances of several combined high order low diffusion schemes with the fifth order WENO scheme by using the lemma.

In this paper, based on the definition of a derivative, a parameter free shock detecting method different from the one of Shen and Zha[15], which is based on the relation between the smoothness indicators, is proposed. A class of high order shock-capturing hybrid algorithms are constructed. Numerical examples show that the new methods are accurate, efficient and robust.

2 Shock Detector

Based on the definition of a derivative, the necessary and sufficient conditions for differentiability of a function f at x_i are:

(1) Both $\lim\limits_{\Delta x_i^+ \to 0} \dfrac{f_i^+ - f_i}{\Delta x_i^+}$ and $\lim\limits_{\Delta x_i^- \to 0} \dfrac{f_i - f_i^-}{\Delta x_i^-}$ exist,

(2) $\lim\limits_{\Delta x_i^+ \to 0} \dfrac{f_i^+ - f_i}{\Delta x_i^+} = \lim\limits_{\Delta x_i^- \to 0} \dfrac{f_i - f_i^-}{\Delta x_i^-}$,

where, $\Delta x_i^+ = x_i^+ - x_i$, $\Delta x_i^- = x_i - x_i^-$.

2.1 Non-differentiability Indicator at Three-points Stencil

Based on above conditions, for the numerical computation, a sufficient condition for non-differentiability(it is generalized to the spatial interval Δx_i, which can not be infinitesimal) of the function f at stencil $S^3 = (x_{i-1}, x_i, x_{i+1})$ is proposed as following, Let

$$\beta_0 = (f_{i+1} - f_i), \quad \beta_1 = (f_i - f_{i-1}), \quad \tau = |\beta_0^2 - \beta_1^2|, \tag{1}$$

If

$$\tau > min(\beta_0^2, \beta_1^2) \tag{2}$$

then f is non-differentiable at stencil S^3. Note since β_0^2 and β_1^2 are used to detect the non-differentiable point, a sharp peak point, which is a non-differentiable point, may be numerically treated as a local extreme point.

Let $\Delta x = \Delta x^+ = \Delta x^-$, using the method of reduction to absurdity, it is easy to prove above conclusion. In fact, if f is smooth at stencil S^3, by using Taylors expansion series, we have

$$\begin{cases} \beta_0 = f_i'\Delta x + \frac{1}{2}f_i''\Delta x^2 + \frac{1}{3}f_i'''\Delta x^3 + \cdots \\ \beta_1 = f_i'\Delta x - \frac{1}{2}f_i''\Delta x^2 + \frac{1}{3}f_i'''\Delta x^3 + \cdots \end{cases} \tag{3}$$

it can be seen that τ is always an infinitesimal of a higher order than β_0^2 and β_1^2.

2.2 Non-differentiability Indicator at Five-points Stencil

This can be generalized to the five-points stencil $S^5 = (x_{i-2}, x_{i-1}, x_i, x_{i+1}, x_{i+2})$. Let

$$\beta_0 = \frac{1}{2}(f_{i-2} - 4f_{i-1} + 3f_i), \quad \beta_1 = \frac{1}{2}(-3f_i + 4f_{i+1} - f_{i+2}), \quad \tau = |\beta_0^2 - \beta_1^2| \tag{4}$$

If

$$\tau > min(\beta_0^2, \beta_1^2) \tag{5}$$

then f is non-differentiable at stencil S^5.

$\beta_0/\Delta x$ and $\beta_1/\Delta x$ can be regarded as the second order left and right approximation of the first derivative of f, respectively.

Similar as the prove of the indicator at three-points stecil, suppose that f is differential at stencil S^5, by using by using Taylors expansion series, we have

$$\begin{cases} \beta_0 = f_i'\Delta x - \frac{2}{3}f_i'''\Delta x^3 + \frac{6}{4!}f_i^{(4)}\Delta x^4 + \cdots \\ \beta_1 = f_i'\Delta x - \frac{2}{3}f_i'''\Delta x^3 - \frac{6}{4!}f_i^{(4)}\Delta x^4 + \cdots \end{cases} \tag{6}$$

Hence, if $f_i' \neq 0$, there is

$$\tau = |f_i' f_i^{(4)}|\Delta x^5 + O(\Delta x^6)$$

while

$$\beta_k^2 = (f_i')^2\Delta x^2 + O(\Delta x^4), \ k = 0, 1.$$

that means τ is an infinitesimal with three order (about Δx) higher than β_k^2. This also shows that, under the case with $f_i' \neq 0$, the indicator with five points is more accurate than that with three points. If $f_i' = 0$, then τ is also an infinitesimal of a higher order than β_k^2.

2.3 Shock Detector

For the numerical calculation of the hyperbolic conservation laws, even if the solution contains discontinuity, the first order derivative should be discretized. Thus, for applications of computational fluid dynamics, the condition (2) or (5), can be used as the shock detector at the corresponding stencil.

3 The Numerical Algorithm

Considering the following hyperbolic conservation equation,

$$\frac{\partial u}{\partial t} + \frac{\partial f}{\partial x} = 0 \tag{7}$$

Its semi-discretized form can be written as

$$\frac{\partial u_i}{\partial t} = -\frac{1}{\Delta x}(h_{i+1/2} - h_{i-1/2}) \tag{8}$$

where $h_{i+1/2}$ is the numerical flux function.

3.1 The Linear Difference Scheme

The general form of linear difference scheme is

$$\sum_{l=-p}^{q} \gamma_l h_{i+1/2+l} = \sum_{k=-m}^{n} a_k f_{i+k} \tag{9}$$

where $\gamma_0 \neq 0$. If $\gamma_l = 0 (l \neq 0)$, then $h_{i+1/2}$ is the traditional explicit finite difference scheme; otherwise, $h_{i+1/2}$ is the compact finite difference scheme. The parameters p, q, m, n and the coefficients γ_l and a_k can be obtained according to different requirement and using Taylor expansion.

3.2 The WENO Scheme

The high order linear difference schemes always generate spurious numerical oscillation if the solution contains large gradient or discontinuity. The weighted essentially non-oscillatory (WENO) schemes have uniform higher order accuracy in smooth region and keep the essentially non-oscillatory properties near shock waves, and are widely used in CFD applications. The numerical flux of the r-th order WENO scheme can be written as

$$h_{i+1/2} = \sum_{k=0}^{r-1} \omega_k q_k \tag{10}$$

where q_k is the rth order approximation of $h_{i+1/2}$ at stencil $S_k^r = (x_{i+k-r+1}, \cdots, x_{i+k})$, the weights ω_k are defined as

$$\omega_k = \frac{\alpha_k}{\sum_{l=0}^{2} \alpha_l}, \quad \alpha_k = \frac{C_k^r}{(IS_k + \epsilon)^p} \tag{11}$$

C_k^r are the ideal weights to make flux (10) be the $(2r-1)-th$ order accurate. The smoothness indicators IS_k are given as

$$IS_k = \sum_{l=1}^{2} \Delta x^{2l-1} \int_{x_{i-1/2}}^{x_{i+1/2}} \left(q_k^{(l)}\right)^2 dx \tag{12}$$

where $q_k^{(l)}$ is the lth-derivative of $q_k(x)$. The parameter ϵ is used to avoid the division by zero. In [16], $\epsilon = 10^{-6}$ and the power $p = 2$ are suggested. Borges et al.[17] proposed new smoothness indicators IS_k^z for the 5th-order WENO scheme,

$$IS_k^z = \frac{IS_k + \epsilon}{IS_k + \tau_5 + \epsilon} \tag{13}$$

where τ_5 is defined as

$$\tau_5 = |IS_0 - IS_2| \tag{14}$$

3.3 Hybrid Algorithm Using the Parameter-free Shock Detector

In [15], Shen and Zha give the following lemma as the discontinuity detector[15]:

Lemma 1. If $\tau_5 > \min(IS_0, IS_1, IS_2)$, then S^5 is a non-smooth stencil.

Then, a generalized finite compact difference is suggested as the following:

(1) A zone containing a discontinuity is detected by using Lemma 1, and the fluxes within this zone including at the zone boundaries are calculated by a WENO scheme.

(2) those smooth point(s) between two zones containing discontinuities(or between boundary point and discontinuous interface)are defined as a compact stencil, and a compact scheme is used to calculate the numerical fluxes on the compact stencil.

In [18], the above algorithm is generalized by using different high order schemes to substitute the compact scheme used in step (2), and their performances are compared numerically.

In this paper, except the shock detector (2) or (5) is used, the constructing procedure of a hybrid algorithm is the same as above mentioned procedure. For completeness, the procedure of the high order low diffusion hybrid scheme is described as following,

Procedure of the High Order Low Dissipation Hybrid Algorithm

BEGIN

Step 0. calculate $h_{1/2}$ and $h_{N+1/2}$ using boundary formula

Step 1. M=1 ! looking for starting and ending points for smooth region using the shock detector

start_point(M)=1 ! smooth region starting point

DO i=1,N-1

calculate τ

IF $\tau > min(\beta_0^2, \beta_1^2)$ THEN

end_point(M)=i ! smooth region ending point

M=M+1

start_point(M)=i+1

calculate $h_{i+1/2}$ using WENO scheme:

$$h_{i+\frac{1}{2}} = \sum_{k=0}^{2} \omega_k q_k \tag{15}$$

END IF

END DO

end_point(M)=N

Step 2. DO k=1,M ! calculate fluxes on smooth region k using a high order scheme

DO j=start_point(k), end_point(k)-1

calculate the right hand side $d_{i+1/2}$

END DO

solve the equations(general form)

$$\alpha h_{i-1/2} + \gamma h_{i+1/2} + \beta h_{i+3/2} = d_{i+1/2}, \tag{16}$$

where, i =start_point(k), $\cdots$, end_point(k)-1.

END DO

END

Note: in step (2), if the compact scheme is used, then the fluxes on the discontinuity zones obtained from step (1) are automatically used as the internal boundary fluxes.

4 Numerical Examples

In this paper, the 4th order Runge-Kutta-type method[19] is used for the time marching of the governing equations. For simplicity, the simple abbreviation is used to represent the different schemes, for example, 3p-4Pade-W5 denotes the three-points stencil shock detecor (2), 4th-order Pade compact scheme in smooth region and 5th-order WENO scheme for the shock stencil are used.

4.1 Linear transport equation

The linear transport equation is used to test the accuracy of the new scheme.

$$\frac{\partial u}{\partial t} + \frac{\partial u}{\partial x} = 0, \ -1 < x < 1 \tag{17}$$
$$u(x,0) = u_0(x), \ periodic$$

(1)

$$u_0(x) = sin(2\pi x) \tag{18}$$

Table 1 gives the error and accuracy. It can be seen that, 3p-4Pade-W5 scheme is only 3rd-order accurate for the L_∞ error, while 5p-6Pade-W5 is uniformly 6th-order accurate. The reason is that, for the three-points stencil detector, τ is only a first-order infinitesimal of β_0 and β_1 in smooth region, while for the five-points stencil detector, τ is a third-order infinitesimal of β_0 and β_1. Compared Table 1 and the results given in [18], for the smooth solution, the five-points stencil detector proposed in this paper and the detector in Ref.[15] give the same results, except the former is slightly more accurate than the latter at coarse grid.

(2)

$$u_0(x) = \begin{cases} \frac{1}{6}(G(x,\beta,z-\delta) + G(x,\beta,z+\delta) + 4G(x,\beta,z)), & -0.8 \le x \le -0.6, \\ 1, & -0.4 \le x \le -0.2, \\ 1 - |10(x-0.1)|, & 0 \le x \le 0.2, \\ \frac{1}{6}(F(x,\alpha,\alpha-\delta) + F(x,\alpha,\alpha+\delta) + 4F(x,\alpha,a)), & 0.4 \le x \le 0.6, \\ 0, & otherwise \end{cases} \tag{19}$$

Table 1: Accuracy on $u_t + u_x = 0$ with $u_0(x) = sin(2\pi x)$, t=1

Scheme	N	L_∞ error	L_∞ order	L_1 error	L_1 order
WENO-Z	40	0.3423E-03		0.2102E-03	
	80	0.1021E-04	5.067	0.6308E-05	5.059
	160	0.3142E-06	5.022	0.1980E-06	4.994
	320	0.9792E-08	5.004	0.6206E-08	4.995
	640	0.3058E-09	5.001	0.1943E-09	4.998
3p-4Pade-W5	40	0.5560E-03		0.2889E-03	
	80	0.5730E-04	3.278	0.2489E-04	3.537
	160	0.6825E-05	3.070	0.1801E-05	3.789
	320	0.7551E-06	3.176	0.1205E-06	3.902
	640	0.8799E-07	3.101	0.7712E-08	3.965
5p-6Pade-W5	40	0.1000E-03		0.3167E-04	
	80	0.2446E-05	5.353	0.7561E-06	5.388
	160	0.4242E-07	5.850	0.1189E-07	5.991
	320	0.6903E-09	5.941	0.1817E-09	6.032
	640	0.1092E-10	5.983	0.2903E-11	5.968

Same as in Ref.[16], the constants for this case are taken as $a = 0.5$, $z = -0.7$, $\delta = 0.005$, $\alpha = 10$, and $\beta = log2/36\delta^2$. The solution contains a smooth combination of Gaussians, a square wave, a sharp triangle wave, and a half ellipse.

The results at $t = 8$ with 200 grid points are shown in Figs. 1 and 2. It can be seen that, 3p-4Pade-W5 and 5p-6Pade-W5 schemes obtain more accurate solution of Gaussians, a square wave, a sharp triangle wave than the WENO-Z scheme. 3p-4Pade-W5 scheme overshoots at the extremum point of the ellipse wave. For comparing, Fig. 3 gives the results of 5p-6Pade-W5 and the method in Ref.[15]. 5p-6Pade-W5 is more accurate than the method in Ref.[15] for all waves. Since the the compact scheme and the WENO scheme used in the two methods are the same, the results indicate that the shock detector of $\tau_5 > min(IS_0, IS_1, IS_2)$ is more strict than the present detector of $\tau > min(\beta_0^2, \beta_1^2)$.

4.2 1D Shock Wave Tube, Shu-Osher Problem

This problem is governed by the one-dimensional Euler equations with following initial condition:

$$(\rho, u, p) = \begin{cases} (3.857143, 2.629369, 10.3333), & when\ x < -4, \\ (1 + \varepsilon sin(5x), 0.0, 1.0), & when\ x \geq -4. \end{cases} \tag{20}$$

where, $\varepsilon = 0.2$. This case represents a Mach 3 shock wave interacting with a sine entropy wave[20]. Steger-Warming flux vector splitting method[21] is used. The results at time $t = 1.8$ with mesh size 300 are plotted in Fig. 4. The "exact" solutions are the numerical solutions of the original WENO-Z scheme with grid points of $N = 4000$. For this case, it can be seen that, the present schemes resolves the wave peaks better than the WENO-Z scheme due to smaller dissipation of a compact scheme.

4.3 Two-dimensional Shock/Shear Layer Interaction

A two-dimensional shock/shear layer interaction problem is solved to demonstrate these schemes for multi-dimensional flows. The two-dimensional Navier-Stokes equations are solved for this problem:

$$\frac{\partial \mathbf{U}}{\partial t} + \frac{\partial \mathbf{E}}{\partial x} + \frac{\partial \mathbf{F}}{\partial y} = \frac{1}{Re}\left[\frac{\partial \mathbf{E_v}}{\partial x} + \frac{\partial \mathbf{F_v}}{\partial y}\right] \tag{21}$$

where

$$\mathbf{U}=\begin{bmatrix}\rho\\ \rho u\\ \rho v\\ \rho e\end{bmatrix},\mathbf{E}=\begin{bmatrix}\rho u\\ \rho u^2+p\\ \rho uv\\ u(\rho e+p)\end{bmatrix},\mathbf{F}=\begin{bmatrix}\rho v\\ \rho uv\\ \rho v^2+p\\ v(\rho e+p)\end{bmatrix},\mathbf{E_v}=\begin{bmatrix}0\\ \tau_{xx}\\ \tau_{xy}\\ u\tau_{xx}+v\tau_{xy}+q_x\end{bmatrix},\mathbf{F}=\begin{bmatrix}0\\ \tau_{xy}\\ \tau_{yy}\\ u\tau_{xy}+v\tau_{yy}+q_y\end{bmatrix},$$

where $\tau_{xx}=\mu(\frac{4}{3}\frac{\partial u}{\partial x}-\frac{2}{3}\frac{\partial v}{\partial y})$, $\tau_{xy}=\mu(\frac{\partial v}{\partial x}+\frac{\partial u}{\partial y})$, $\tau_{xy}=\mu(\frac{4}{3}\frac{\partial v}{\partial y}-\frac{2}{3}\frac{\partial u}{\partial x})$.

$p=(\gamma-1)(\rho e-\rho(u^2+v^2)/2)$, $\gamma=1.4$.

An oblique shock with angle $\beta=12^o$ is made to impact on a spatially developing mixing layer at an initial convective Mach number of 0.5. The computation domain is taken to be $[x,y]=[0,200]\times[-20,20]$. The inflow is specified with a hyperbolic tangent profile,

$$u=2.5+0.5tanh(2y) \tag{22}$$

For the upper stream inflow, $\rho_u=1.6374$, $p_u=0.3327$; for the lower stream inflow, $\rho_l=0.3626$, $p_l=0.3327$. The upper boundary condition is taken from the flow properties behind the oblique shock. The lower wall uses a slip condition.

Fluctuations are added to the v-component of velocity of the inflow as

$$v'=\sum_{k=1}^{2}a_k cos(2\pi kt/T+\phi_k)exp(-y^2/b) \tag{23}$$

with period $T=\lambda/u_c$, wavelength $\lambda=30$, convective velocity $u_c=2.68$, $b=10$, $a_1=a_2=0.05$, $\phi_1=0$ and $\phi_2=\pi/2$.

The Prandtl number is set to 0.72, and the Reynolds number is chosen to be 500. The viscosity μ is calculated by using Sutherland formula. The 4th-order central difference scheme[22] is used for the viscous terms. The uniform grid, 321×81, is used. The time step is taken as follows[2]:

$$\Delta t=\delta\frac{\Delta t_x\Delta t_y}{\Delta t_x+\Delta t_y},\ with\ \Delta t_x=\frac{\Delta x}{max_{i,j}(|u_{i,j}|+c_{i,j})},\ \Delta t_y=\frac{\Delta y}{max_{i,j}(|v_{i,j}|+c_{i,j})} \tag{24}$$

where $\delta=0.5$ is the CFL number.

The Steger-Warming flux vector splitting method[21] is used to calculate the interface fluxes. The density contours are shown in Fig. 5. Due to only the 4th-order Pade scheme is used in smooth regions, 3p-4Pade-W5 resolves the structures of last four vortices not so clear as the WENO-Z (5th-order accurate in smooth regions) scheme. However, 5p-6Pade-W5 obtains vortex structures with significantly higher resolution than the WENO-Z scheme.

4.4 Rayleigh-Taylor instability

This problem has been simulated by many authors, e.g. [23], [24] and [25], to test the numerical dissipation of various high order shock capturing schemes. The initial conditions are

$$(\rho,u,v,p)=\begin{cases}(2,\ 0,\ -0.025\alpha cos(8\pi x),\ 2y+1) & if\ 0\le y<1/2\\ (1,\ 0,\ -0.025\alpha cos(8\pi x),\ y+3/2) & if\ 1/2\le y\le 1\end{cases} \tag{25}$$

where, $\alpha=\sqrt{\gamma p/\rho}$ is the sound speed, the ratio of specific heats $\gamma=5/3$. This problem represents the interface instability between fluids with different densities when an acceleration is directed from heavy fluid to light one. The gravitational effect is introduced by adding ρ and ρv to the right hand side of the y-momentum and the energy equations, respectively. Reflective boundary conditions are imposed for the left and right boundaries, and $(\rho,u,v,p)=(1,0,0,2.5)$ and $(\rho,u,v,p)=(2,0,0,1)$ are set as top and

bottom boundary conditions, respectively. The computational domain is $[0, 1/4] \times [0, 1]$, and the simulation time is $t = 1.95$.

As analyzed in [24, 25], due to the invisid Euler equation is solved, the details of the complex structures due to the physical instability are related to the specific form of numerical viscosity of the scheme. From the density contours ploted in Fig. 6, it can be seen that, the present method with coarse meshes of 61×241 can obtain the comparable solution of WENO-Z scheme with meshes of 121×481. The different instability structures between the present method and the method developed in [15] show that the different shock indicators can generate different numerical viscosity. The difference is more obvious with the refined meshes.

5 Conclusions

In this paper, based on the definition of a derivative, a new shock detecting method without any artificial parameter is proposed. The new shock detector is used with a high order accuracy low dissipation shock-capturing algorithm, in which the high order WENO scheme is used at the shock stencil determined by the shock detecting method and the high order compact scheme is used at the smooth stencils. Hence, the new algorithm has both the non-oscillatory property of WENO scheme and high order low dissipation of compact scheme. Numerical examples show that the new method is accurate, efficient and robust.

6 Acknowledgment

This work was supported by the National Natural Science Foundation of China under Grant Nos. 11272325 and 11272324.

References

[1] N. A. Adams, K. Shariff, "A High-Resolution Hybrid Compact-ENO Scheme for Shock-Turbulence Interaction Problems," *Journal of Computational Physics*, vol. 127, pp. 27–51, 1996.

[2] S. Pirozzoli, "Conservative hybrid compact-WENO schemes for shock-turbulence interaction," *J.Comput.Phys.*, vol. 178, pp. 81–117, 2002.

[3] Yu-Xin Ren, Miao'er Liu, Hanxin Zhang, "A characteristic-wise hybrid compact-WENO scheme for solving hyperbolic conservation laws," *Journal of Computational Physics*, vol. 192, pp. 365–386, 2003.

[4] Qiang Zhou, Zhaohui Yao, Feng He, M.Y. Shen, "A new family of high-order compact upwind difference schemes with good spectral resolution," *Journal of Computational Physics*, vol. 227, pp. 1306–1339, 2007.

[5] Y.-Q. Shen, G.-W. Yang, Z. Gao, "High-resolution finite compact difference schemes for hyperbolic conservation laws," *J.Comput.Phys.*, vol. 216, pp. 114–137, 2006.

[6] Y.-Q. Shen, G.-W. Yang, "Hybrid finite compact-WENO schemes for shock calculation," *International Journal for Numerical Methods in Fluids*, vol. 53, pp. 531–560, 2007.

[7] D. J. Hill, D. I. Pullin, " Hybrid tuned center-difference-WENO method for large eddy simulations in the presence of strong shock," *Journal of Computational Physics*, vol. 194, pp. 435–450, 2004.

[8] C. Pantano, R. Deiterding, D.J. Hill and D.I. Pullin, "A low numerical dissipation patch-based adaptive mesh refinement method for large-eddy simulation of compressible flows," *J.Comput.Phys.*, vol. 221, pp. 63–87, 2007.

[9] B. Costa, W.S.Don, , "High order hybrid central-WENO finite difference scheme for conservation laws," *Journal of Computational Physics*, vol. 204, pp. 209–218, 2007.

[10] A. Harten, "ENO schemes with subcell resolution," *Journal of Computational Physics*, vol. 83, pp. 148–184, 1989.

[11] H. C. Yee, N. D. Sandham, M. J. Djomehri, "Low-Dissipative High-Order Shock-Capturing Methods Using Characteristic-Based Filters," *Journal of Computational Physics*, vol. 150, pp. 199–238, 1999.

[12] H.C. Yee, B. Sjogreen, "Development of low dissipative high order filter schemes for multiscale Navier-Stokes/MHD systems," *Journal of Computational Physics*, vol. 225, pp. 910–934, 2007.

[13] C. Bogey, N. de Cacqueray, C. Bailly, "A shock-capturing methodology based on adaptative spatial filtering for high-order non-linear computations," *Journal of Computational Physics*, vol. 228, pp. 1447–1465, 2009.

[14] H. M. Darian, V. Esfahanian, K. Hejranfar, "A shock-detecting sensor for filtering of high-order compact finite difference schemes," *Journal of Computational Physics*, vol. 230, pp. 494–514, 2011.

[15] Y.-Q Shen, G.-C Zha, "Generalized finite compact difference scheme for shock/complex flowfield interaction," *Journal of Computational Physics*, vol. 230, pp. 4419–4436, 2011.

[16] G.-S. Jiang, C.-W. Shu, "Efficient implementation of weighted ENO schemes," *J.Comput.Phys.*, vol. 126, pp. 202–228, 1996.

[17] R. Borges, M. Carmona, B. Costa, W.S. Don, "An improved weighted essentially non-oscillatory scheme for hyperbolic conservation laws," *Journal of Computational Physics*, vol. 227, pp. 3191–3211, 2008.

[18] Y. Q. Shen, G. Z. Zha, G. W. Yang, Z. Gao, "Comparisons of high order hybrid schemes using a parameter-free discontinuity detector." 42nd AIAA Fluid Dynamics Conference and Exhibt, New Orleans, 2012.

[19] C.-W. Shu, O. Osher, "Efficient implementation of essentially non-oscillatory shock capturing schemes," *Journal of Computational Physics*, vol. 77, pp. 439–471, 1988.

[20] C.-W. Shu, O. Osher, "Efficient Implementation of Essentially Non-Oscillatory Shock Capturing Schemes, II," *Journal of Computational Physics*, vol. 83, pp. 32–78, 1989.

[21] J. L. Steger, R. F. Warming, "Flux vector splitting of the inviscid gasdynamic equations with application to finite-difference methods," *Journal of Computational Physics*, vol. 40, pp. 263–293, 1981.

[22] Y.-Q. Shen, G.-Z. Zha, X.-Y. Chen , "High order conservative differencing for viscous terms and the application to vortex-induced vibration flows," *Journal of Computational Physics*, vol. 228, pp. 8283–8300, 2009.

[23] Y. N. Young, H. Tufo, A. Dubey, R. Rosner, "On the miscible Rayleigh-Taylor instability: two and three dimensions," *Journal of Fluid Mechanics*, vol. 447, pp. 377–408, 2001.

[24] J. Shi, Y. T. Zhang, C.W. Shu, "Resolution of high order WENO schemes for complicated flow structures," *Journal of Computational Physics*, vol. 186, pp. 690–696, 2003.

[25] Z.F. Xu and C.-W. Shu, "Anti-diffusive flux corrections for high order finite difference WENO schemes," *J.Comput.Phys.*, vol. 205, pp. 458–485, 2005.

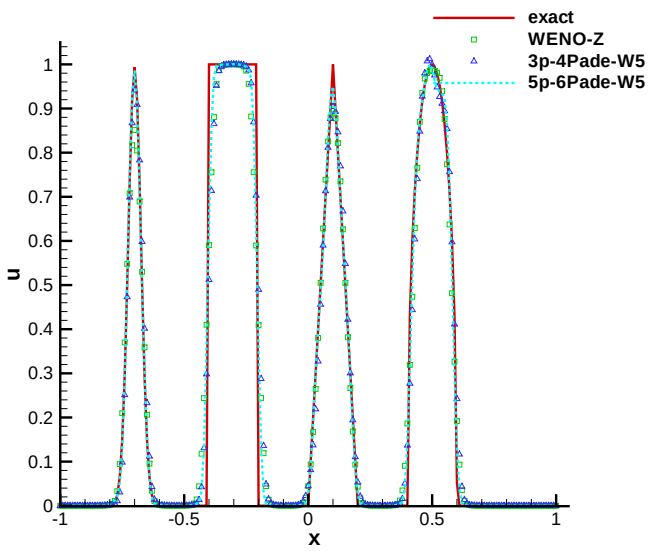

Figure 1: Linear transport equation, problem 2, $t = 8$

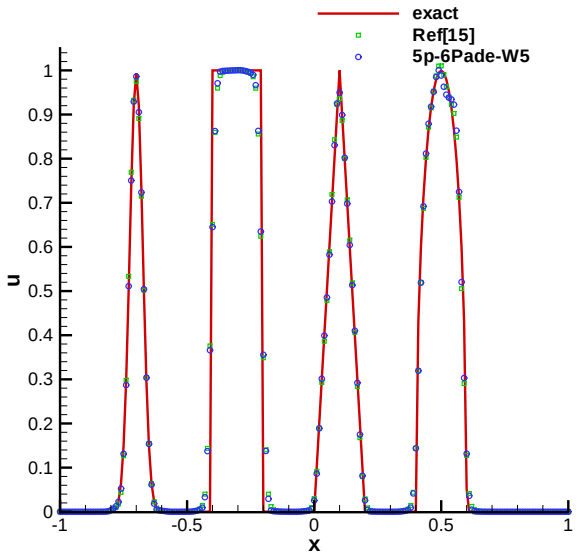

Figure 3: Linear transport equation, problem 2, $t = 8$

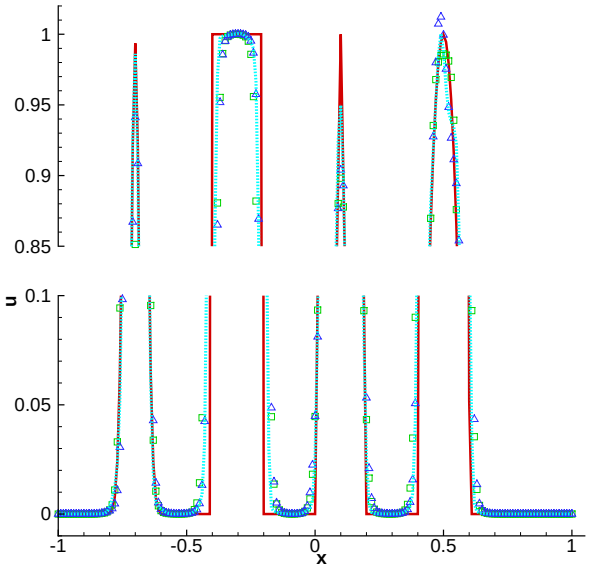

Figure 2: Locally enlarged plot of Fig. 1

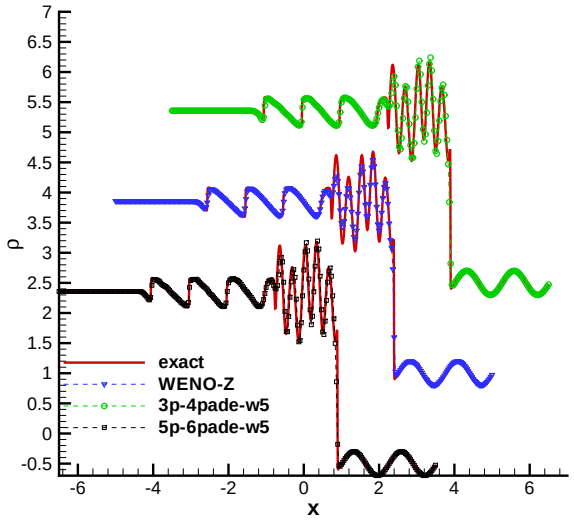

Figure 4: Shu-Osher problem, $t = 1.8$

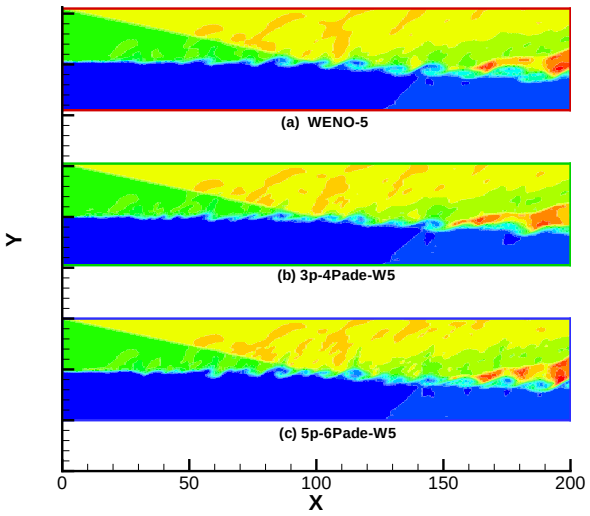

Figure 5: Density contours of the shock wave/shear interaction, $t = 120$.

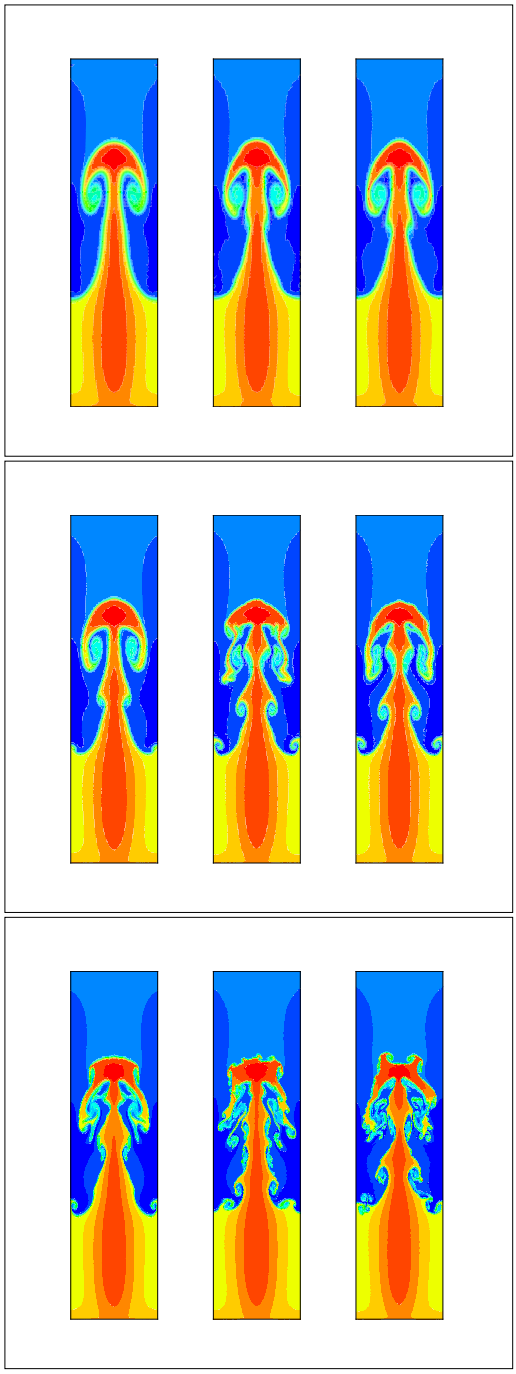

Figure 6: Rayleigh-Taylor instability, $t = 1.95$. From left to right: WENO-Z, Shen and Zha[15], present method. From top to bottom: 61×241, 121×481, 481×481.